A tandem activity-based sensing and labeling strategy enables imaging of transcellular hydrogen peroxide signaling

Hidefumi Iwashita[a], Erika Castillo[b], Marco S. Messina[a], Raymond A. Swanson[b,c], and Christopher J. Chang[a,d,e,1]

[a]Department of Chemistry, University of California, Berkeley, CA 94720; [b]Department of Neurology, University of California, San Francisco and San Francisco Veterans Affairs Medical Center, San Francisco, CA 94143; [c]Neurology Service, San Francisco Veterans Affairs Health Care System, San Francisco, CA 94121; [d]Department of Molecular and Cell Biology, University of California, Berkeley, CA 94720; and [e]Helen Wills Neuroscience Institute, University of California, Berkeley, CA 94720

Edited by Catherine J. Murphy, University of Illinois at Urbana–Champaign, Urbana, IL, and approved January 7, 2021 (received for review September 2, 2020)

Reactive oxygen species (ROS) like hydrogen peroxide (H_2O_2) are transient species that have broad actions in signaling and stress, but spatioanatomical understanding of their biology remains insufficient. Here, we report a tandem activity-based sensing and labeling strategy for H_2O_2 imaging that enables capture and permanent recording of localized H_2O_2 fluxes. Peroxy Green-1 Fluoromethyl (PG1-FM) is a diffusible small-molecule probe that senses H_2O_2 by a boronate oxidation reaction to trigger dual release and covalent labeling of a fluorescent product, thus preserving spatial information on local H_2O_2 changes. This unique reagent enables visualization of transcellular redox signaling in a microglia–neuron coculture cell model, where selective activation of microglia for ROS production increases H_2O_2 in nearby neurons. In addition to identifying ROS-mediated cell-to-cell communication, this work provides a starting point for the design of chemical probes that can achieve high spatial fidelity by combining activity-based sensing and labeling strategies.

fluorescent hydrogen peroxide probe | activity-based sensing | redox signaling | oxidative stress | NADPH oxidase

Reactive oxygen species (ROS) are a family of small molecules that play broad roles in physiology and pathology (1–6). In this context, hydrogen peroxide (H_2O_2) is an ROS that is both a source of oxidative stress and a potent signaling molecule. H_2O_2 has been shown to regulate cell growth, differentiation, migration, and death pathways. Indeed, beyond its classical roles in phagocytic killing of pathogens during immune response (7–9), production of H_2O_2 via superoxide by NADPH oxidase (Nox) enzymes in nonphagocytic cells (10) can trigger signaling events that contribute to a diverse array of physiological processes including neural activity and long-term potentiation (11–14) and depression, stem cell growth and proliferation (15–17), circadian rhythms (18–20), and wound healing (21, 22).

Owing to its transient and reactive nature, the vast majority of studies on H_2O_2 signaling have focused on intracellular communication events. Indeed, despite its small size and relatively nonpolar nature, H_2O_2 is not freely diffusible through membranes, and its entry into cells is tightly regulated, as our laboratory (23) and others (24–27) have identified specific isoforms of aquaporin water channels as endogenous mediators of H_2O_2 transport. As such, roles for H_2O_2 in transcellular communication remain insufficiently understood. This gap in fundamental knowledge is due in part to limitations in chemical tools to visualize integrated H_2O_2 activity that can retain spatial information over larger and/or more complex cell populations. Indeed, there have been recent elegant developments in sensing platforms and probe design (28–31). In terms of H_2O_2 sensing, conventional small-molecule fluorescent probes for H_2O_2 can quickly access sites of local H_2O_2 elevations but can also diffuse away after ROS detection (32–43), diluting signal-to-noise responses. Likewise, traditional fluorescent protein–based indicators that reversibly respond to H_2O_2 can be localized by genetic encoding but are limited to studies within a microscope's field of view (44–48) and do not provide a permanent signal.

Here we report a dual activity-based sensing and labeling strategy for selective and sensitive fluorescence detection of H_2O_2 with the ability to capture and record spatial information over defined time scales. Peroxy Green-1 Fluoromethyl (PG1-FM, Scheme 1) promotes a tandem boronate oxidation sensing and quinone methide labeling sequence upon reaction with H_2O_2 to covalently trap the probe in cells and afford a permanent stain that preserves spatial information on localized H_2O_2 fluxes. PG1-FM is capable of monitoring elevations in endogenous H_2O_2 production in live cells and is useful for both microscopy and flow cytometry assays. As an example of its utility, we use this probe to visualize transcellular ROS signaling in a microglia–neuron coculture system. This approach presages further opportunities for combining chemical sensing and labeling strategies to decipher biology with improved spatial fidelity.

Results and Discussion

Design and Synthesis of PG1-FM. The design of PG1-FM combines the reliable boronate trigger established by our laboratory for activity-based sensing of H_2O_2 (32, 34) with a pendant fluoromethyl

Significance

Hydrogen peroxide is a ubiquitous reactive oxygen species (ROS) with diverse signaling and stress contributions, but its transient and mobile nature makes it challenging to study in living systems. Here we report a tandem activity-based sensing and labeling strategy for capture and permanent recording of localized H_2O_2 fluxes by fluorescence imaging. Application of this technology enables direct visualization of ROS transport in cell-to-cell communication using a microglia–neuron coculture model to monitor cell-specific elevations in H_2O_2 levels. In addition to revealing a fundamental contribution of ROS to transcellular signaling, this work presages further opportunities to combine dual chemical sensing and labeling approaches to probe biology with improved spatial fidelity.

Author contributions: H.I., E.C., R.A.S., and C.J.C. designed research; H.I., E.C., and M.S.M. performed research; H.I. contributed new reagents/analytic tools; H.I., E.C., M.S.M., R.A.S., and C.J.C. analyzed data; and H.I. and C.J.C. wrote the paper.

The authors declare no competing interest.

This article is a PNAS Direct Submission.

[1]To whom correspondence may be addressed. Email: chrischang@berkeley.edu.

This article contains supporting information online at https://www.pnas.org/lookup/suppl/doi:10.1073/pnas.2018513118/-/DCSupplemental.

Published February 23, 2021.

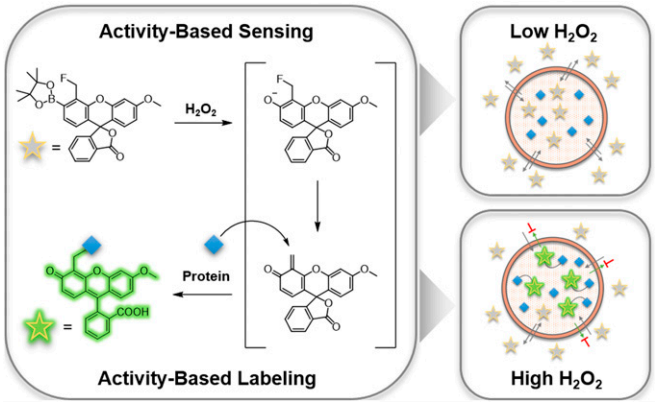

Scheme 1. Design and chemical structure of PG1-FM, a dual activity-based sensing and labeling probe for fluorescence H_2O_2 detection.

group ortho to this cage that serves as a latent quinone methide species for proximal covalent labeling upon H_2O_2-mediated boronate-to-phenol conversion. This tandem sensing and labeling strategy affords the ability to trap the probe at the site of H_2O_2 reactivity (Scheme 1). We were inspired by elegant studies by Urano and colleagues on the use of fluoromethyl arenes as latent electrophiles for cell-specific labeling and killing purposes (49–51) with single-cell resolution. In the absence of H_2O_2, the fluoromethyl aryl boronate probe is freely diffusible throughout the cell and between cells as it is membrane permeable. However, upon reaction with H_2O_2, conversion of the boronate to the corresponding phenol triggers fluoride elimination to generate a highly reactive quinone methide electrophile, which, when generated intracellularly, can be locally captured by proximal protein–based nucleophiles, leaving a fluorescent product covalently labeled at the site of the activity-based sensing reaction. A key advance enabled by the design feature of this approach compared to conventional small-molecule fluorophores is that it minimizes background signal from extracellular H_2O_2 reactivity and entry of the oxidized probe into cells, in contrast to previous probes that rely on esterase trapping and give signal from dyes both before and after reaction with H_2O_2 (15, 23). Indeed, in this tandem sensing and labeling strategy, oxidized dye products would be largely quenched by either water or extracellular protein nucleophiles and rendered membrane impermeable, where they can be readily washed away from the cell. This feature results in enhanced signal-to-noise responses from localized intracellular H_2O_2 fluxes. As such, this tandem activity-based sensing and labeling strategy uniquely enables visualization of H_2O_2 with the ability to retain and record permanent spatial information in both live- and fixed-cell settings by covalent modification. Moreover, this dual activity-based sensing and labeling approach should be generally applicable to the design of a broader array of probes for other biological analytes of interest. The synthesis of PG1-FM was accomplished from methoxyfluorescein (52) through a five-step reaction sequence (Scheme 2). Briefly, formylation of methoxyfluorescein 1 with hexamethylenetetramine under acidic conditions gave aldehyde 2. The phenol group of aldehyde 2 was converted into a trifluoromethanesulfonyl moiety with N-phenyl-bis(trifluoromethanesulfonimide), $PhN(Tf)_2$, to yield compound 3. The formyl group of 3 was reduced by sodium triacetoxyborohydride in presence of acetic acid, followed by the fluorination of the hydroxymethyl moiety with DAST to give compound 4. Finally, boronation of trifluoromethanesulfonyl moiety with a palladium-mediated cross-coupling reaction afforded PG1-FM (Scheme 2). Peroxyfluor-2 (PF2) is an activity-based sensing probe developed in our group which is responsive toward H_2O_2 but lacks a proximal fluoromethyl group and is therefore unable to undergo biomolecule labeling (53). As such, PF2 is used throughout this study as a nontrappable comparison to PG1-FM (Scheme 2). Over the course of our studies, the Hamachi group reported similar cell-trappable reagents and applied them to fluorescence microscopy and proteomic techniques (54).

PG1-FM Is a Dual Activity-Based Sensing and Labeling Probe with Hydrogen Peroxide and Protein Substrates. We first evaluated the in vitro response of PG1-FM to hydrogen peroxide in aqueous solution buffered to physiological pH. As expected by its activity-based sensing boronate trigger, the probe exhibited a clear fluorescence enhancement after treatment with H_2O_2 and converted to a fluorescent product that undergoes subsequent hydrolysis with H_2O by liquid chromatography analysis (Fig. 1*A* and *SI Appendix*, Fig. S3). Moreover, PG1-FM gave a highly selective response for H_2O_2 over other biologically relevant ROSand reactive nitrogen species congeners (Fig. 1*B* and *SI Appendix*, Fig. S1). PG1-FM, with its dual sensing and labeling mechanism, gives a selective signal for hydrogen peroxide with little signal for peroxynitrite under these conditions. We note that some boronates appear to react much faster with peroxynitrite than hydrogen peroxide and vice versa in spectroscopic experiments in buffer solution, but in cells the levels of hydrogen peroxide are generally much higher and more sustained than peroxynitrite, as the latter has a shorter lifetime (6, 55–57). As such, it is critical to do control experiments in cells where if hydrogen peroxide is the key ROS, then inhibiting Nox would reduce signal as opposed to peroxynitrite, where inhibiting nitric oxide synthase would reduce signal (36). In the models tested here, the combination of chemical inhibition of Nox with diphenyleneiodonium (DPI) or a hydrogen peroxide scavenger (ebselen) along with a genetic Nox knockout support hydrogen peroxide detection. To establish activity-based labeling of PG1-FM in a H_2O_2-dependent manner, we incubated the probe with bovine serum albumin (BSA) as a model protein substrate in the presence or absence of H_2O_2, and the reactions were analyzed by sodium dodecyl sulphate-polyacrylamide gel electrophoresis (SDS-PAGE). A fluorescent BSA-associated band was observed only under conditions with H_2O_2, consistent with H_2O_2-dependent labeling of the protein with the dye (Fig. 1*C*) (32, 34). These data establish that PG1-FM is a H_2O_2-responsive and H_2O_2-selective fluorescent probe that can undergo a secondary labeling reaction with a model protein upon activity-based sensing. Additionally, SDS-PAGE analysis of experiments in which whole-cell (MFP 231) lysate was treated with varying concentrations of H_2O_2 (200 to 1,000 μM) in the presence of PG1-FM (10 μM) indicated the presence of multiple fluorescent bands. This experiment demonstrates that PG1-FM modifies proteins in a nonselective manner (*SI Appendix*, Fig. S2). Similar experiments in the absence of H_2O_2 or in the presence of H_2O_2 (1,000 μM) and PF2 (10 μM) indicated that no protein labeling had occurred (*SI Appendix*, Fig. S2).

PG1-FM Can Monitor Elevations in H_2O_2 Levels in Live Cells with Exogenous Peroxide Treatment. We next assessed the ability of PG1-FM for visualizing changes in H_2O_2 levels in live cells with exogenous H_2O_2 treatment. HeLa cells were prestained with PG1-FM (10 μM), treated with H_2O_2 (100 μM) or vehicle control, washed, and imaged. PG1-FM exhibits minor cellular toxicity in the presence of H_2O_2 when compared with H_2O_2-treated HeLa cells in the absence of PG1-FM (*SI Appendix*, Fig. S4). We observed that the probe loads evenly throughout the cell and responds to elevations in H_2O_2 in both HeLa and MCF10A cells (*SI Appendix*, Figs. S5 and S6). These data show that the dual activity-based sensing and labeling strategy is viable for live-cell H_2O_2 imaging. However, as the overall activity-based sensing

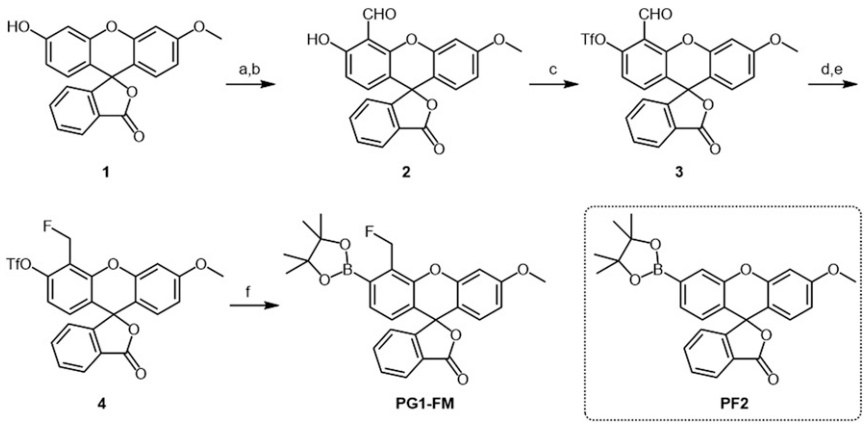

Scheme 2. Synthesis of PG1-FM. Reagents and conditions are the following: (*A*) hexamethylenetetramine, TFA, 90 °C, 16 h; (*B*) H_2O, 95 °C, 1 h; (*C*) N-phenyl-bis(trifluoromethanesulfonimide), Cs_2CO_3, MeCN, room temperature (r.t.), 1 h; (*D*) $NaBH(OAc)_3$, AcOH, THF/MeOH, 1 h; (*E*) DAST, CH_2Cl_2, –20 °C to r.t., 1 h; and (*F*) Bis(pinacolato)diboron, $Pd(dppf)Cl_2$, KOAc, Dioxane, 80 °C, 3 h. PF2 is used throughout this study as a control compound which is responsive toward H_2O_2 but does not undergo biomolecule labeling.

and labeling scheme is irreversible, the relative levels of H_2O_2 before and after stimulation can be monitored, but the probe strategy has limitations in the ability to monitor multiple reversible redox cycling events.

PG1-FM Can Image Endogenous H_2O_2 Production in Live Cells during Oxidative Stress or Redox Signaling. We next utilized PG1-FM for imaging endogenous H_2O_2 fluxes produced by multiple types of cell models under various stimulation conditions. Our first set of experiments along these lines evaluated the performance of the probe under conditions of oxidative stress induced by paraquat treatment. HeLa cells were stimulated with or without paraquat (1 mg/mL) for 24 h to induce ROS and oxidative stress, followed by staining with PG1-FM for 30 min, washing, and imaging. HeLa cells exposed to paraquat showed patent H_2O_2-dependent fluorescence increases compared to untreated counterparts as observed by confocal microscopy (Fig. 2*A*). Because the probe is cell trappable, we verified the observed fluorescence enhancements using flow cytometry (Fig. 2 *B* and *C*), highlighting its utility in this analytical method as well.

We next applied PG1-FM to detect endogenous H_2O_2 produced by growth factor stimulation in A431 cells, a skin cancer cell line that has high expression levels of the epidermal growth factor receptor (EGFR) and is known to generate H_2O_2 by stimulation with epidermal growth factor (EGF) through Nox activity (36, 58). Owing to the fast generation of H_2O_2 by EGF stimulation relative to paraquat, A431 cells were stained with PG1-FM first and then treated with 1 μg/mL of EGF or vehicle control for 30 min, washed, and imaged. Confocal microscopy images show a clear increase in fluorescence for EGF-stimulated A431 cells over control counterparts (Fig. 3*A*). Moreover, addition of DPI as a broad-spectrum Nox inhibitor or ebselen as a general antioxidant quencher of H_2O_2 inhibited H_2O_2-induced enhancements in PG1-FM fluorescence (Fig. 3*B*).

Finally, we tested the ability of PG1-FM to monitor H_2O_2 production in RAW 264.7 macrophages. This mouse leukemia macrophage cell model is known to generate H_2O_2 via superoxide by stimulation with phorbol 12-myristate 13-acetate (PMA), which activates Nox through a protein kinase C–dependent pathway (59). PMA (1 μg/mL)-treated cells for 60 min showed higher PG1-FM fluorescence relative to control cells by both confocal microscopy

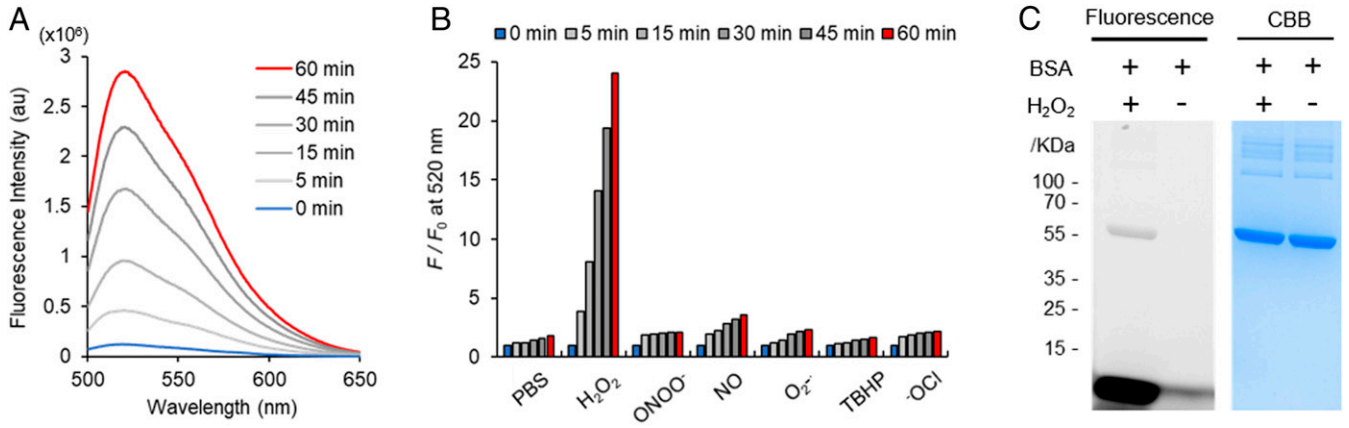

Fig. 1. Fluorescence responses and activity-based sensing and labeling properties of PG1-FM. (*A*) Activity-based sensing fluorescence responses of 1 μM PG1-FM to 25 μM H_2O_2. Data were acquired in phosphate-buffered saline (PBS) (pH 7.4) at 37 °C with 488 nm excitation. (*B*) Fluorescence responses of 1 μM PG1-FM toward biologically relevant competing ROS and reactive nitrogen species. Data were acquired in PBS (pH 7.4) at 37 °C with 488 nm excitation. (*C*) H_2O_2-dependent activity-based labeling of PG1-FM to BSA. A solution of BSA (0.5 mg/mL) and PG1-FM (1 μM) in PBS (pH 7.4) was incubated with or without H_2O_2 (100 μM) and analyzed by SDS-PAGE gel.

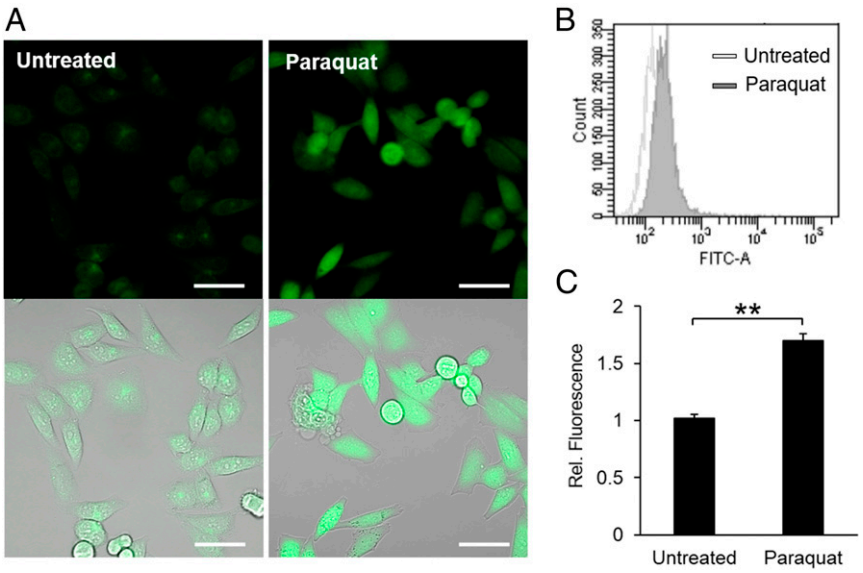

Fig. 2. PG1-FM imaging of endogenous H_2O_2 generation in live HeLa cells under oxidative stress conditions stimulated by paraquat. (*A*) Confocal microscopy images of HeLa cells treated with or without paraquat (1 mg/mL) for 24 h, stained with PG1-FM (10 μM) for 1 h, washed twice with HBSS, and imaged. (Scale bar: 50 μm.) (*B*) Flow cytometry analysis of the cells treated with or without paraquat using PG1-FM using same conditions as *A*. (*C*) Flow cytometric data quantified with mean value. $^{**}P < 0.01$.

and flow cytometry assays (Fig. 4). Moreover, as observed for the EGF-stimulated A431 models, fluorescence increases are blocked by DPI or ebselen (Fig. 4 *A*–*C*). Taken together, the collective results establish that the dual activity-based sensing and labeling probe PG1-FM is effective for detecting exogenous and endogenous changes in H_2O_2 levels across a range of cell models and stimulation conditions by both microscopy and flow cytometry.

PG1-FM Enables Direct Visualization of Transcellular H_2O_2 Communication in a Microglia–Neuron Coculture Model. With data showing that PG1-FM can monitor H_2O_2 produced for intracellular signaling, we then proceeded to apply this reagent to studies of transcellular redox signaling using a microglia–neuron coculture system. This culture model recapitulates neuronal injury mediated by microglial activation in diverse disease processes (59–62). Microglia are specialized resident macrophages in the central nervous system, and they can be activated to produce H_2O_2 via superoxide by stimulation with lipopolysaccharide (LPS) and interferon-gamma (IFN-γ) (63). $p47^{phox}$ (phox: phagocyte oxidase) is known to be mandatory for production of superoxide and H_2O_2 in microglia cells. Neurons do not respond to LPS in this manner, so the coculture system provides a means of visualizing transfer of ROS from one cell type (microglia) to another (neurons) by selective activation of microglia.

Microglia and neuron monocultures and microglia–neuron cocultures were prepared and treated with LPS (500 ng/mL) and IFN-γ (50 ng/mL) overnight and then incubated with PG1-FM (10 μM) for 1 h. PG1-FM localization in microglia and neurons was identified using the MAP2 as a neuronal marker and Iba-1 as

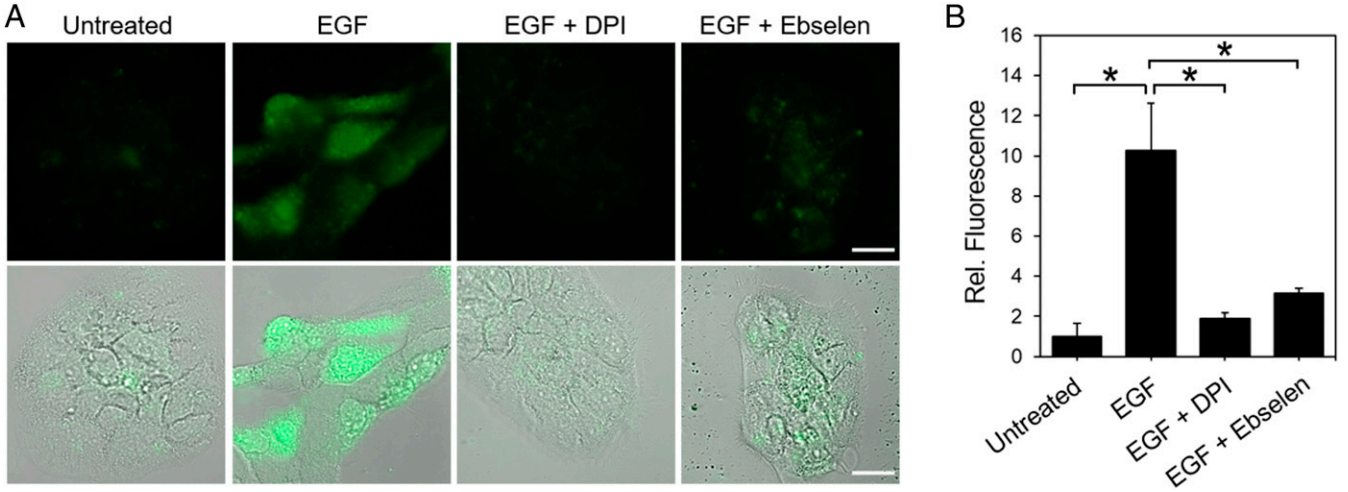

Fig. 3. PG1-FM imaging of endogenous H_2O_2 generation in live A431 cells under redox signaling conditions with EGF stimulation. (*A*) Confocal microscopy (*Top*) and overlaid brightfield (*Bottom*) images of A431 cells stained with PG1-FM (10 μM) and then treated with EGF (1 μg/mL) or vehicle control for 30 min, washed and imaged, or first pretreated with Nox inhibitor DPI (5 μM) or antioxidant ebselen (5 μM) for 30 min in HBSS solution before PG1-FM staining and EGF stimulation. (*B*) Quantification of experiments. (Scale bar: 20 μm.) $^{*}P < 0.05$.

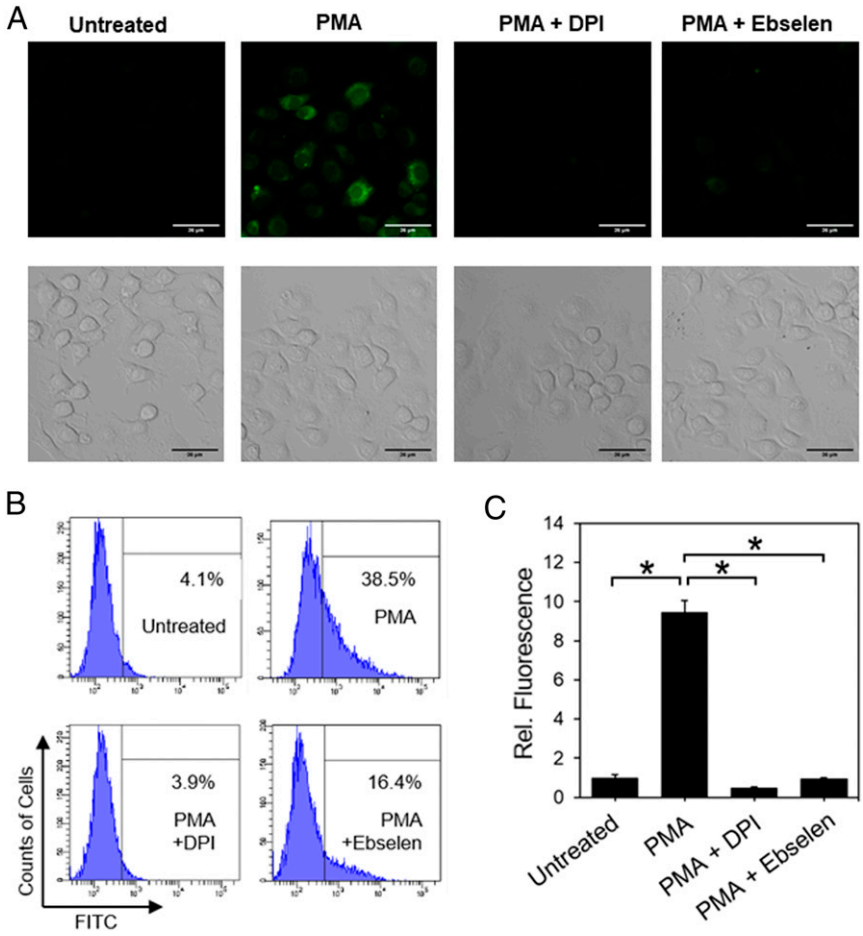

Fig. 4. PG1-FM imaging of endogenous H_2O_2 generation in live RAW264.7 macrophage cells under inflammatory immune response conditions with PMA stimulation. (*A*) Confocal microscopy (*Top*) and brightfield (*Bottom*) images of RAW264.7 macrophages stained with PG1-FM (10 μM) and then treated with PMA (1 μg/mL) or vehicle control for 60 min, washed, and imaged or first pretreated with Nox inhibitor DPI (5 μM) or antioxidant ebselen (5 μM) for 30 min in HBSS solution (250 μL) before replacing the solutions in the wells with a mixture of PG1-FM and PMA in the presence of additional DPI (5 μM) or ebselen in HBSS (5 μM). (*B*) Flow cytometry histograms and (*C*) quantification of mean value fluorescence intensity using PG1-FM under same conditions as *A*. (Scale bar: 36 μm.) *$P < 0.01$.

a microglial marker. Microglial monocultures treated with LPS/IFN-γ showed a striking increase in PG1-FM labeling, whereas neuronal monocultures treated with LPS/IFN-γ did not, as expected (Fig. 5). In contrast, neurons cocultured with microglia showed significant increases in PG1-FM signal fluorescence with LPS/IFN-γ stimulation, indicative of transcellular movement of H_2O_2 from microglia into the neighboring neurons (Fig. 5 *A*–*C* and *SI Appendix*, Fig. S7). Interestingly, neuronal coculture with microglia in the absence of LPS/IFN-γ also led to a small rise in neuronal H_2O_2 levels, with a basal level of activation in the cultured microglia (Fig. 5 *A*–*C* and *SI Appendix*, Fig. S7).

To confirm that the neuronal PG1-FM signal was caused by microglial ROS production, rather than signaling to induce neuronal ROS production, we also performed the coculture studies with $p47^{pho}$ knockout ($p47^{phox-/-}$) microglia cells. These cells are unable to form a functional NOX2 complex and are thus unable to generate H_2O_2, even when stimulated with LPS/IFNγ (*SI Appendix*, Fig. S8). As expected, in the coculture system with neurons and $p47^{phox-/-}$ microglia, neurons labeled with PG1-FM do not show significant fluorescence increases upon stimulation compared to neurons cocultured with wild-type (WT) microglia cells, confirming that the observed elevations in H_2O_2 levels in neurons are dependent on $p47^{phox}$-mediated ROS production in microglia (Fig. 6 *A*–*C*). The observed microglia-mediated increases in neuronal H_2O_2 levels thus establish the ability of PG1-FM to capture and record intracellular H_2O_2 fluxes as well as distinguish H_2O_2-positive cells from H_2O_2-negative cells in complex coculture models with single-cell resolution.

Concluding Remarks

We have presented the design, synthesis, and biological applications of a tandem activity-based sensing and labeling probe strategy for fluorescence imaging of H_2O_2 that enables the ability to provide an integrated recording of H_2O_2 fluxes with permanent retention of spatial resolution. PG1-FM features an activity-based boronate trigger for selective and sensitive H_2O_2 detection coupled to a fluoromethyl moiety that serves as a latent quinone methide source for proximal covalent trapping upon the H_2O_2-mediated conversion of a boronate to phenol on the reporter probe. This unique reagent is capable of monitoring changes in H_2O_2 levels through endogenous sources across a range of cell types and stimulations using both microscopy and flow cytometry, including the direct observation of transcellular redox signaling between microglia and neurons in a coculture model system where selective stimulation of microglia results in rises in intracellular levels of H_2O_2 in neighboring neurons. Microglial ROS production contributes to neuronal injury in neurodegenerative disorders, ischemic stroke, brain trauma, and other settings (59–61), but the transient nature of ROS in living cells has

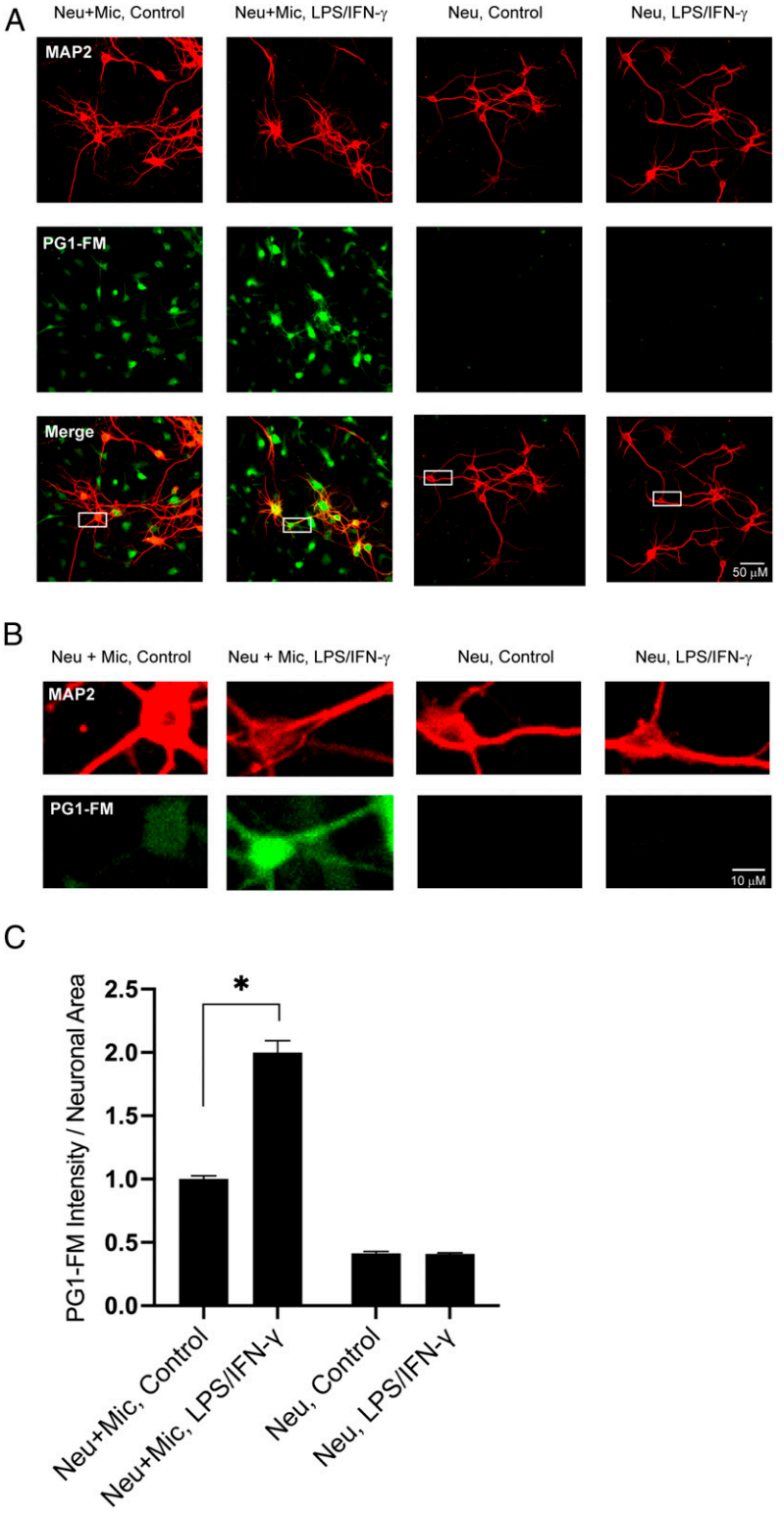

Fig. 5. PG1-FM imaging of transcellular H_2O_2 signaling in microglia–neuron cocultures. (*A*) Representative images of neuronal monocultures and neurons cocultured with microglia. The cultures were treated overnight with 500 ng/mL LPS + 50 ng/mL IFN-γ, incubated with 10 μM PG1-FM (green) for 1 h, and immunostained for the neuronal marker MAP2 (red). (Scale bar: 50 μm.) (*B*) Magnification of boxed areas in merged images in (*A*), showing intraneuronal H_2O_2 signal only in neurons cocultured with microglia and increase in the H_2O_2 signal microglial stimulation by LPS/IFN-γ. (Scale bar: 10 μm.) (*C*) Values plotted as PG1-FM fluorescence intensity within MAP2 positive area; mean ± SEM, normalized to the neuron/microglia control condition. $n = 3$, with 9 to 11 fields in each condition examined per repetition. Neu: neurons, Mic: microglia. $^*P < 0.05$.

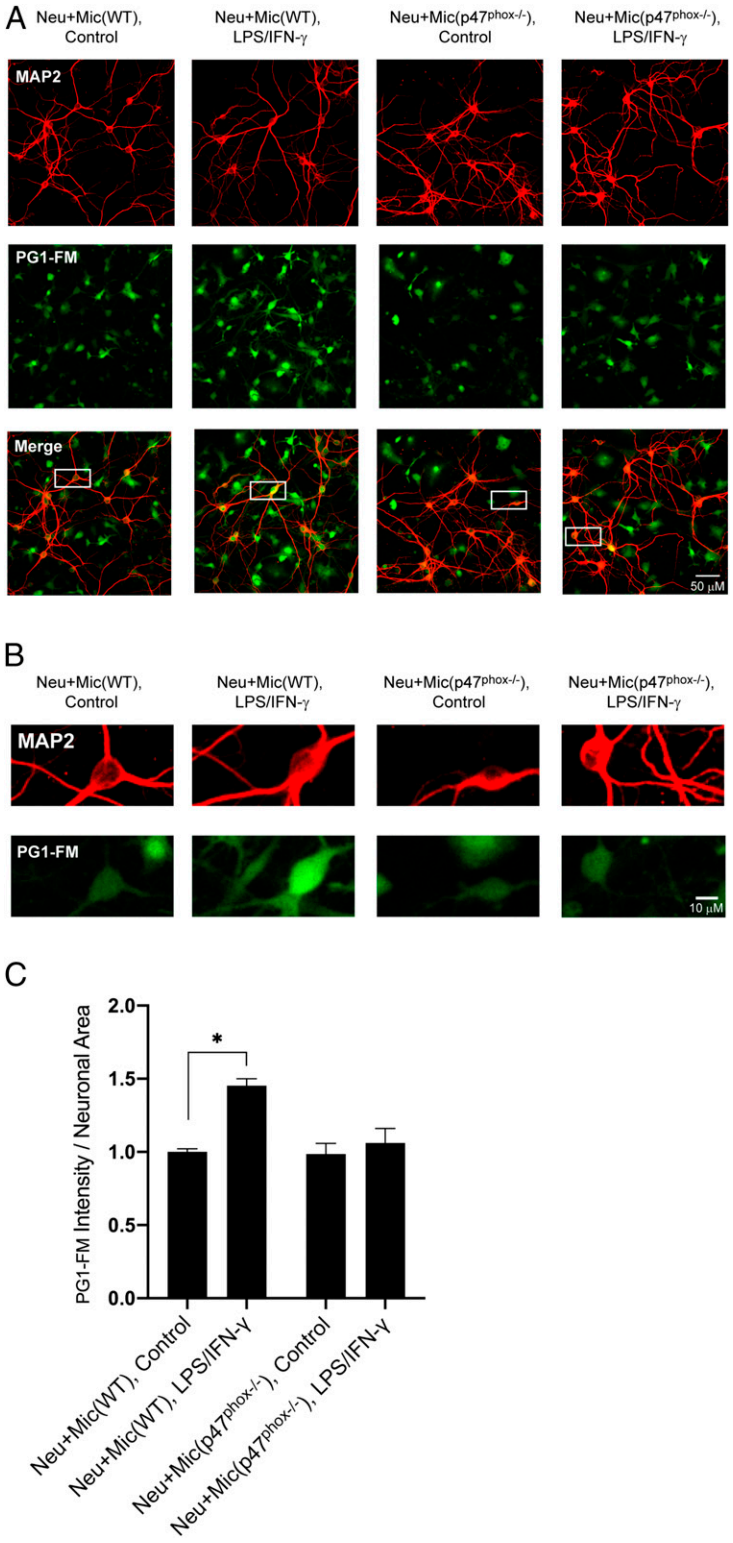

Fig. 6. PG1-FM imaging of transcellular H_2O_2 signaling in neurons cultured with WT microglia and $p47^{phox}$ knockout microglia. (*A*) Representative images of neuron/microglia cocultures treated overnight with 500 ng/mL LPS + 50 ng/mL IFN-γ. Cultures were incubated with 10 μM PG1-FM (green) for 1 h and immunostained for the neuronal marker MAP2 (red). PG1-FM signal was increased in neurons cultured with WT microglia, but not in neurons cultured with $p47^{phox-/-}$ microglia. (Scale bar: 50 μm.) (*B*) Magnification of boxed areas in merged images in *A*. (Scale bar: 10 μM.) (*C*) Values plotted as PG1-FM fluorescence intensity within MAP2 positive area; mean ± SEM, normalized to the neuron/microglia (WT) control condition. $n = 3$, with 8 to 11 fields examined per repetition. Neu: neurons, Mic: microglia. $^*P < 0.05$.

limited efforts to identify temporal and spatial aspects of these processes. Our findings presage opportunities to explore consequences of microglial and other sources of ROS diseasing these and related disorders. By directly visualizing H_2O_2 elevations triggered by transcellular activation, this work reveals a role for H_2O_2, and most certainly other ROS, in cell-to-cell communication more broadly.

On the chemistry side, owing to the variety of available phenol-based fluorophores, the fluoromethyl motif can serve as a latent masked quinone methide to produce probes spanning a palette of colors and additional targeting groups to further increase spatial and temporal resolution. Indeed, beyond applications for PG1-FM and related imaging probes for recording localized and integrated H_2O_2 activity in larger and more complex cell populations, the combination of activity-based sensing and labeling strategies can be applied to a broader range of analytes to decipher new biology (64, 65).

Materials and Methods

Reagents and Instruments. General chemicals were purchased from Tokyo Chemical Industry Co., Aldrich Chemical Co., and Thermo Fisher and were used without purification unless otherwise noted. ^{1}H NMR, ^{13}C NMR, and ^{19}F NMR spectra were recorded using Bruker AVB-400, AVQ-400, and AV-300 spectrometers at the College of Chemistry nuclear magnetic resonance (NMR) Facility at the University of California, Berkeley. Low-resolution electrospray mass spectral analyses were performed using a liquid chromatography-mass spectrometry (LC-MS) (Advion Expression-L Compact MS, electrospray ionization [ESI] source). High-resolution mass spectra were measured at the College of Chemistry Mass Spectrometry Facility at the University of California, Berkeley. Fluorescence spectra were measured using a Photon Technology International Quanta Master 4 L-format scan spectrofluorometer equipped with an LPS-220B 75-W xenon lamp and power supply, A-1010B lamp housing with integrated igniter, switchable 814 photocounting/analog photomultiplier detection unit, and MD5020 motor driver. Fluorescence images were obtained with a Zeiss LSM 880 confocal laser scanning microscopy system, excited at 488 nm using a 500 to 650 nm filter for PG1-FM. Cell viability assay on 96-well plates was performed with a synergy plate reader (BioTek).

Cell Culture. Cells were grown at the UC Berkeley Tissue Culture Facility. HeLa, RAW264.7, and A431 cells were cultured in Dulbecco's Modified Eagle Medium (DMEM) (high glucose) supplemented with 10% fetal bovine serum, GlutaMAX, and non-essential amino acid (NEAA). All cells were maintained in a humidified 5% CO_2 incubator at 37 °C.

Representative Live-Cell Imaging Experiments: HeLa or MCF10A Cells with H_2O_2 Treatment. Cells were washed twice with Hank's Balanced Salt Solution (HBSS) buffer (250 μL) before treatments. Cells were treated with PG1-FM (10 μM) or PF2 (10 μM) in HBSS (250 μL) and placed in a humidified 5% CO_2 incubator at 37 °C for 30 min. The cells were washed with HBSS (250 μL) twice, and treated with H_2O_2 (250 μL, 100 μM in HBSS) and placed in a humidified 5% CO_2 incubator at 37 °C for 60 min. The cells were observed on confocal microscope after washing with HBSS (250 μL) twice.

Representative Live-Cell Imaging Experiments: RAW264.7 Cells with Endogenous Stimulation. RAW264.7 cells were plated on a μ-slide 8-well (ibidi) plate and cultured at 37 °C overnight in a 5% CO_2 incubator. The cells were pretreated with inhibitors, DPI (5 μM), or Ebselen (5 μM) for 30 min in HBSS (250 μL per well). Afterward, the solutions in the wells were replaced with mixtures of PG1-FM (10 μM), PMA (1 μg/mL), and additional DPI or ebselen (5 μM) in HBSS (250 μL per well). The cells were observed on confocal microscope after washing with HBSS twice.

Flow Cytometric Analysis. RAW264.7 cells were plated on a 6-well plate and cultured at 37 °C overnight in a 5% CO_2 incubator. The cells were pretreated with inhibitors, DPI (5 μM), or Ebselen (10 μM), for 30 min in HBSS. Afterward, the cells were coincubated with PG1-FM (5 μM) and PMA (1 μg/mL) with or without DPI or Ebselen. The cells were harvested by 0.05% Trypsin with EDTA, filtered, and analyzed with flow cytometer.

Primary Neuron and Microglia Isolation and Culture. Procedures were approved by the San Francisco Veterans Affairs Medical Center Institutional Animal Care and Use Committee. Primary neuronal cultures were prepared from cortices harvested from embryonic day 18 to 20 C57BL/6 mice. Cell suspensions were prepared from the cortices by papain digestion and trituration, and the isolated cells were plated on poly-D-lysine (PDL)–coated coverslips in Opti-MEM medium (Gibco, 31985) at 4×10^5 cells/mL and allowed to attach for 1 h. Medium was replaced with Neurobasal media (Gibco, 21103049) supplemented with B-27, 2 mM L-glutamine, and 1 mM sodium pyruvate for 7 to 10 d before treatment. Microglia cultures were prepared from postnatal day 0 or 1 C57BL/6 WT or p47^{phox} knockout mice. Cell suspensions were prepared from the cortices by papain digestion and trituration, and the isolated cells were plated on PDL-coated flasks in DMEM (Gibco, A14430) containing 10% fetal bovine serum, 1% penicillin/streptomycin, 5 mM glucose, 2 mM L-glutamine, and 1 mM sodium pyruvate. Medium was renewed the following day to remove cell debris. At day 5, 10 ng/mL Granulocyte-macrophage colony-stimulating factor (Biolegend, 576302) was added to promote microglial proliferation. To collect microglia growing on the top of the confluent astrocyte layer, the flasks were tapped and shaken quickly, and floating cells were collected, centrifuged, and replated in the glia-conditioned medium on PDL-coated plates at a density of 2×10^5 cells/mL or on the top of the neuronal culture at a density of 1×10^5 cells/mL. Cultures were used for further analysis the following day.

Primary Culture Treatments and Labeling with PG1-FM. Microglia, neurons, and microglia–neuron cultures were incubated in HBSS with no phenol red, with or without 500 ng/mL LPS + 50 ng/mL IFN-γ and incubated overnight. Then, 10 μM PG1-FM was directly added to the wells for 1 h and cells were fixed with 4% paraformaldehyde solution.

Immunofluorescence. Fixed cells were permeabilized with 0.3% triton-X for 10 min then incubated for 1 h with blocking buffer. Cells were incubated overnight at 4 °C with primary antibodies diluted in blocking buffer, and the antibodies used were mouse anti-MAP2 (Millipore, MAB3418, 1:1,000), goat anti-Iba1 (Abcam, ab107159, 1:500), or rabbit anti-Iba1 (Fujifilm, 019–19741, 1:500). After washing, cells were incubated 1 h with Alexa Fluor–conjugated secondary antibodies that do not interfere with the PG1-FM dye signal. Images were acquired using a Zeiss Spinning Disk Confocal microscope. Immunofluorescence intensity of PG1-FM was calculated per number of cells, for microglia culture images or per MAP2-positive area of individual cells, for coculture images using the ImageJ/Fiji software. Photographs and data analysis were done by an individual who was blinded to the experimental conditions.

Statistics. All experiments were performed in triplicate and analyzed with GraphPad Prism 8, and data were expressed as mean ± SEM. Comparisons between groups of treatments were carried out using one-way analysis of variance followed by Tukey's multiple comparison test. Data were considered statistically significant when $P < 0.05$.

Data Availability. All study data are included in the article and/or *SI Appendix*.

ACKNOWLEDGMENTS. This work was supported by the NIH (GM139245, ES28096, and ES4705 to C.J.C.) and by the Department of Veterans Affairs (1IO1 BX004884 to R.A.S.). We also thank The Agilent-Berkeley Synthetic Biology Institute program for support (to C.J.C). M.S.M. thanks the University of California, Berkeley, President's and Aduro-Berkeley Postdoctoral Fellowships for funding. We thank Alison Killilea, Carissa Tasto, and Molly Fischer of the University of California Berkeley Cell Culture Facility for expert technical assistance.

1. B. D'Autréaux, M. B. Toledano, ROS as signalling molecules: Mechanisms that generate specificity in ROS homeostasis. *Nat. Rev. Mol. Cell Biol.* **8**, 813–824 (2007).
2. C. C. Winterbourn, Reconciling the chemistry and biology of reactive oxygen species. *Nat. Chem. Biol.* **4**, 278–286 (2008).
3. H. M. Cochemé *et al*., Measurement of H_2O_2 within living Drosophila during aging using a ratiometric mass spectrometry probe targeted to the mitochondrial matrix. *Cell Metab.* **13**, 340–350 (2011).
4. M. Schieber, N. S. Chandel, ROS function in redox signaling and oxidative stress. *Curr. Biol.* **24**, R453–R462 (2014).
5. D. Reichmann, W. Voth, U. Jakob, Maintaining a healthy proteome during oxidative stress. *Mol. Cell* **69**, 203–213 (2018).
6. H. Sies, D. P. Jones, Reactive oxygen species (ROS) as pleiotropic physiological signalling agents. *Nat. Rev. Mol. Cell Biol.* **21**, 363–383 (2020).
7. M. C. Dinauer, S. H. Orkin, R. Brown, A. J. Jesaitis, C. A. Parkos, The glycoprotein encoded by the X-linked chronic granulomatous disease locus is a component of the neutrophil cytochrome b complex. *Nature* **327**, 717–720 (1987).
8. B. D. Volpp, W. M. Nauseef, R. A. Clark, Two cytosolic neutrophil oxidase components absent in autosomal chronic granulomatous disease. *Science* **242**, 1295–1297 (1988).

9. R. A. Clark *et al*., Genetic variants of chronic granulomatous disease: Prevalence of deficiencies of two cytosolic components of the NADPH oxidase system. *N. Engl. J. Med.* **321**, 647–652 (1989).
10. J. D. Lambeth, NOX enzymes and the biology of reactive oxygen. *Nat. Rev. Immunol.* **4**, 181–189 (2004).
11. A. Kamsler, M. Segal, Hydrogen peroxide modulation of synaptic plasticity. *J. Neurosci.* **23**, 269–276 (2003).
12. M. V. Tejada-Simon *et al*., Synaptic localization of a functional NADPH oxidase in the mouse hippocampus. *Mol. Cell. Neurosci.* **29**, 97–106 (2005).
13. A. M. Brennan *et al*., NADPH oxidase is the primary source of superoxide induced by NMDA receptor activation. *Nat. Neurosci.* **12**, 857–863 (2009).
14. R. De Pasquale, T. F. Beckhauser, M. S. Hernandes, L. R. Giorgetti Britto, LTP and LTD in the visual cortex require the activation of NOX2. *J. Neurosci.* **34**, 12778–12787 (2014).
15. B. C. Dickinson, J. Peltier, D. Stone, D. V. Schaffer, C. J. Chang, Nox2 redox signaling maintains essential cell populations in the brain. *Nat. Chem. Biol.* **7**, 106–112 (2011).
16. J. E. Le Belle *et al*., Proliferative neural stem cells have high endogenous ROS levels that regulate self-renewal and neurogenesis in a PI3K/Akt-dependant manner. *Cell Stem Cell* **8**, 59–71 (2011).
17. C. Xu, J. Luo, L. He, C. Montell, N. Perrimon, Oxidative stress induces stem cell proliferation via TRPA1/RyR-mediated Ca^{2+} signaling in the *Drosophila* midgut. *eLife* **6**, e22441 (2017).
18. J. S. O'Neill, A. B. Reddy, Circadian clocks in human red blood cells. *Nature* **469**, 498–503 (2011).
19. R. S. Wible *et al*., NRF2 regulates core and stabilizing circadian clock loops, coupling redox and timekeeping in *Mus musculus*. *eLife* **7**, e31656 (2018).
20. J. F. Pei *et al*., Diurnal oscillations of endogenous H_2O_2 sustained by $p66^{Shc}$ regulate circadian clocks. *Nat. Cell Biol.* **21**, 1553–1564 (2019).
21. P. Niethammer, C. Grabher, A. T. Look, T. J. Mitchison, A tissue-scale gradient of hydrogen peroxide mediates rapid wound detection in zebrafish. *Nature* **459**, 996–999 (2009).
22. A. Hervera *et al*., Reactive oxygen species regulate axonal regeneration through the release of exosomal NADPH oxidase 2 complexes into injured axons. *Nat. Cell Biol.* **20**, 307–319 (2018).
23. E. W. Miller, B. C. Dickinson, C. J. Chang, Aquaporin-3 mediates hydrogen peroxide uptake to regulate downstream intracellular signaling. *Proc. Natl. Acad. Sci. U.S.A.* **107**, 15681–15686 (2010).
24. G. P. Bienert *et al*., Specific aquaporins facilitate the diffusion of hydrogen peroxide across membranes. *J. Biol. Chem.* **282**, 1183–1192 (2007).
25. M. Dynowski, G. Schaaf, D. Loque, O. Moran, U. Ludewig, Plant plasma membrane water channels conduct the signalling molecule H_2O_2. *Biochem. J.* **414**, 53–61 (2008).
26. O. Rodrigues *et al*., Aquaporins facilitate hydrogen peroxide entry into guard cells to mediate ABA- and pathogen-triggered stomatal closure. *Proc. Natl. Acad. Sci. U.S.A.* **114**, 9200–9205 (2017).
27. C. Rodrigues *et al*., Human aquaporin-5 facilitates hydrogen peroxide permeation affecting adaption to oxidative stress and cancer cell migration. *Cancers (Basel)* **11**, 932 (2019).
28. J. García-Calvo *et al*., Fluorescent membrane tension probes for super-resolution microscopy: Combining mechanosensitive cascade switching with dynamic-covalent ketone chemistry. *J. Am. Chem. Soc.* **142**, 12034–12038 (2020).
29. N. Panyain *et al*., Discovery of a potent and selective covalent inhibitor and activity-based probe for the deubiquitylating enzyme UCHL1, with antifibrotic activity. *J. Am. Chem. Soc.* **142**, 12020–12026 (2020).
30. G. J. Brighty *et al*., Using sulfuramidimidoyl fluorides that undergo sulfur(VI) fluoride exchange for inverse drug discovery. *Nat. Chem.* **12**, 906–913 (2020).
31. W. Wang, K. J. Wu, K. Vellaisamy, C. H. Leung, D. L. Ma, Peptide-conjugated long-lived theranostic imaging for targeting GRPr in cancer and immune cells. *Angew. Chem. Int. Ed. Engl.* **59**, 17897–17902 (2020).
32. A. R. Lippert, G. C. Van de Bittner, C. J. Chang, Boronate oxidation as a bioorthogonal reaction approach for studying the chemistry of hydrogen peroxide in living systems. *Acc. Chem. Res.* **44**, 793–804 (2011).
33. T. F. Brewer, F. J. Garcia, C. S. Onak, K. S. Carroll, C. J. Chang, Chemical approaches to discovery and study of sources and targets of hydrogen peroxide redox signaling through NADPH oxidase proteins. *Annu. Rev. Biochem.* **84**, 765–790 (2015).
34. M. C. Y. Chang, A. Pralle, E. Y. Isacoff, C. J. Chang, A selective, cell-permeable optical probe for hydrogen peroxide in living cells. *J. Am. Chem. Soc.* **126**, 15392–15393 (2004).
35. H. Maeda *et al*., Fluorescent probes for hydrogen peroxide based on a non-oxidative mechanism. *Angew. Chem. Int. Ed.* **43**, 2389–2391 (2004).
36. E. W. Miller, O. Tulyathan, E. Y. Isacoff, C. J. Chang, Molecular imaging of hydrogen peroxide produced for cell signaling. *Nat. Chem. Biol.* **3**, 263–267 (2007).
37. A. R. Lippert, K. R. Keshari, J. Kurhanewicz, C. J. Chang, A hydrogen peroxide-responsive hyperpolarized ^{13}C MRI contrast agent. *J. Am. Chem. Soc.* **133**, 3776–3779 (2011).
38. M. Abo *et al*., Development of a highly sensitive fluorescence probe for hydrogen peroxide. *J. Am. Chem. Soc.* **133**, 10629–10637 (2011).
39. Y. Hitomi, T. Takeyasu, T. Funabiki, M. Kodera, Detection of enzymatically generated hydrogen peroxide by metal-based fluorescent probe. *Anal. Chem.* **83**, 9213–9216 (2011).
40. S. Ye, J. J. Hu, D. Yang, Tandem payne/dakin reaction: A new strategy for hydrogen peroxide detection and molecular imaging. *Angew. Chem. Int. Ed. Engl.* **57**, 10173–10177 (2018).
41. S. Ye *et al*., A highly selective and sensitive chemiluminescent probe for realtime monitoring of hydrogen peroxide in cells and animals. *Angew. Chem. Int. Ed.* **59**, 1–6 (2020).
42. K. J. Bruemmer, S. W. M. Crossley, C. J. Chang, Activity-based sensing: A synthetic methods approach for selective molecular imaging and beyond. *Angew. Chem. Int. Ed. Engl.* **59**, 13734–13762 (2020).
43. D. Pham *et al*., Fluorogenic probe using a mislow-evans rearrangement for real-time imaging of hydrogen peroxide. *Angew. Chem. Int. Ed. Engl.* **59**, 17435–17441 (2020).
44. V. V. Belousov *et al*., Genetically encoded fluorescent indicator for intracellular hydrogen peroxide. *Nat. Methods* **3**, 281–286 (2006).
45. K. N. Markvicheva *et al*., A genetically encoded sensor for H_2O_2 with expanded dynamic range. *Bioorg. Med. Chem.* **19**, 1079–1084 (2011).
46. D. S. Bilan *et al*., HyPer-3: A genetically encoded $H_{(2)}O_{(2)}$ probe with improved performance for ratiometric and fluorescence lifetime imaging. *ACS Chem. Biol.* **8**, 535–542 (2013).
47. M. Gutscher *et al*., Proximity-based protein thiol oxidation by H_2O_2-scavenging peroxidases. *J. Biol. Chem.* **284**, 31532–31540 (2009).
48. B. Morgan *et al*., Real-time monitoring of basal H_2O_2 levels with peroxiredoxin-based probes. *Nat. Chem. Biol.* **12**, 437–443 (2016).
49. T. Doura *et al*., Detection of lacZ-positive cells in living tissue with single-cell resolution. *Angew. Chem. Int. Ed. Engl.* **55**, 9620–9624 (2016).
50. H. Ito *et al*., Red-shifted fluorogenic substrate for detection of lacZ-positive cells in living tissue with single-cell resolution. *Angew. Chem. Int. Ed. Engl.* **57**, 15702–15706 (2018).
51. M. Chiba *et al*., Activatable photosensitizer for targeted ablation of lacZ-positive cells with single-cell resolution. *ACS Cent. Sci.* **5**, 1676–1681 (2019).
52. J. Zhang, Y.-Q. Sun, J. Liu, Y. Shi, W. Guo, A fluorescent probe for the biological signaling molecule H2S based on a specific H2S trap group. *Chem. Commun. (Camb.)* **49**, 11305–11307 (2013).
53. B. C. Dickinson, C. Huynh, C. J. Chang, A palette of fluorescent probes with varying emission colors for imaging hydrogen peroxide signaling in living cells. *J. Am. Chem. Soc.* **132**, 5906–5915 (2010).
54. H. Zhu *et al*., Imaging and profiling of proteins under oxidative conditions in cells and tissues by hydrogen-peroxide-responsive labeling. *J. Am. Chem. Soc.* **142**, 15711–15721 (2020).
55. A. Sikora, J. Zielonka, M. Lopez, J. Joseph, B. Kalyanaraman, Direct oxidation of boronates by peroxynitrite: Mechanism and implications in fluorescence imaging of peroxynitrite. *Free Radic. Biol. Med.* **47**, 1401–1407 (2009).
56. L. Wu *et al*., Reaction-based fluorescent probes for the detection and imaging of reactive oxygen, nitrogen, and sulfur species. *Acc. Chem. Res.* **52**, 2582–2597 (2019).
57. S. Carballal, S. Bartesaghi, R. Radi, Kinetic and mechanistic considerations to assess the biological fate of peroxynitrite. *Biochim. Biophys. Acta* **1840**, 768–780 (2014).
58. C. Yik-Sham Chung, G. A. Timblin, K. Saijo, C. J. Chang, Versatile histochemical approach to detection of hydrogen peroxide in cells and tissues based on puromycin staining. *J. Am. Chem. Soc.* **140**, 6109–6121 (2018).
59. M. L. Block, L. Zecca, J.-S. Hong, Microglia-mediated neurotoxicity: Uncovering the molecular mechanisms. *Nat. Rev. Neurosci.* **8**, 57–69 (2007).
60. M. A. Yenari, T. M. Kauppinen, R. A. Swanson, Microglial activation in stroke: Therapeutic targets. *Neurotherapeutics* **7**, 378–391 (2010).
61. S. Hickman, S. Izzy, P. Sen, L. Morsett, J. El Khoury, Microglia in neurodegeneration. *Nat. Neurosci.* **21**, 1359–1369 (2018).
62. A. I. Faden, J. Wu, B. A. Stoica, D. J. Loane, Progressive inflammation-mediated neurodegeneration after traumatic brain or spinal cord injury. *Br. J. Pharmacol.* **173**, 681–691 (2016).
63. L. Qin *et al*., NADPH oxidase mediates lipopolysaccharide-induced neurotoxicity and proinflammatory gene expression in activated microglia. *J. Biol. Chem.* **279**, 1415–1421 (2004).
64. J. Ohata *et al*., An activity-based methionine bioconjugation approach to developing proximity-activated imaging reporters. *ACS Cent. Sci.* **6**, 32–40 (2020).
65. S. Lee *et al*., Activity-based sening with a metal-directed acyl imidazole strategy reveals cell type-dependent pools of labile brain copper. *J. Am. Chem. Soc.* **142**, 14993–15003 (2020).